Effects of chemical reaction, Soret and Dufour number on unsteady MHD mixed convection flow in the forward stagnation region of a rotating sphere in a porous medium

B.R.Sharma and Debozani Borgohain

Abstract - Soret and Dufour effects on unsteady MHD heat and mass transfer of a chemically reacting, heat absorbing/ generating fluid in the forward stagnation region of a rotating sphere in a porous medium are investigated. The governing non linear partial differential equations are transformed into non dimensional non linear ordinary differential equations using a similarity transformation and are solved numerically by using MATLAB's built in solver bvp4c. Comparisons with previously published work are performed and found to be in excellent agreement. Graphical results are presented to show the influence of the Dufour number, Soret number, porosity parameter, order of the chemical reaction, heat source parameter and dimensionless chemical reaction parameter. It is concluded that the Soret number, Dufour number, porosity parameter and the order of the chemical reaction play a crucial role on the heat and mass transfer.

Keywords - Heat and Mass transfer; MHD; stagnation region; porous medium; rotating sphere; Dufour and Soret effects; chemical reaction.

1. INTRODUCTION

Heat and mass transfer in rotating systems is of considerable interest due to its occurrence in many industrial, engineering and geothermal applications such as nuclear reactors, design of rotating machinery, gas turbines, shielding of rotating bodies, atmospheric and oceanic circulations, filtration, various propulsion devices for space vehicles, missiles, satellites and aircraft, power transformers, vortex chambers and in the modeling of many geophysical vortices [1, 2]. Chemical reaction between a foreign mass and the fluid occurs in many industrial applications such as polymer production, the manufacturing of ceramics or glassware, formation and dispersion of fog, damage of crops due to freezing, distribution of temperature and moisture over groves of fruit trees and so on. Chemical reactions are either homogeneous or heterogeneous processes. The reaction is homogeneous, if it occurs uniformly through a given phase. In well mixed system, it takes place in the solution while a heterogeneous reaction occurs at the interface i.e. in a restricted region or within the boundary of a phase.

- *B. R. Sharma, Professor, Department of Mathematics, Dibrugarh University, Dibrugarh - 786004, Assam, India. E-mail: bishwaramsharma@yahoo.com*
- *Debozani Borgohain, Research Scholar, Department of Mathematics, Dibrugarh University, Dibrugarh - 786004, Assam, India. E-mail: debozanigemini@yahoo.com*

2. RELATED WORK

Magnetohydrodynamic flow and heat transfer in porous and non-porous geometries have been investigated by many researchers such as Sparrow and Cess [3], Riley [4], Raptis and Kafoussias [5], Raptis and Singh [6], Raptis [7], Hossain [8], Kafoussias [9], Takhar and Ram [10], Chamkha [11] and so on. Sharma et al.[12] discussed the influence of chemical reaction, heat source, Soret and Dufour effects on separation of a binary fluid mixture in MHD natural convection flow in porous media. Sharma et al. [13] investigated the influence of the order of chemical reaction and Soret effect on mass transfer of a binary fluid mixture over a stretching tube embedded in a porous media. Influence of chemical reaction, Soret and Dufour effects on heat and mass transfer of a binary fluid mixture in porous medium over a rotating disk was discussed by Sharma and Borgohain [14]. Sharma and Borgohain [15] studied the Soret and Dufour effects on chemically reacting MHD mixed convection flow from a rotating vertical cone in a porous medium

Many researchers Siekann [16], Chao et. al. [17], Lee et. al. [18], Kumari and Nath [19, 20] have discussed on mixed convection flow and heat transfer over a rotating sphere. Chen et. al. [21] used the Keller box scheme to discuss steady mixed or free convection flow over stationary spheres. Takhar et. al [22] studied the unsteady free convection flow in the stagnation point region of a rotating sphere. Takhar and Nath [23] presented a self-similar solution for unsteady flow in the stagnation point region of a rotating sphere with a magnetic field. A self similar solution for unsteady mixed convection boundary layer flow in the forward stagnation point region of a rotating sphere where the free stream

velocity and the angular velocity of the rotating sphere vary continuously with time was reported by Anilkumar and Roy [24]. Rashad et. al [25] investigated the effect of chemical reaction on heat and mass transfer by mixed convection flow about a solid sphere in a saturated porous media. Chamkha et al. [26] analyzed unsteady MHD heat and mass transfer in the forward stagnation region of a rotating sphere.

The present paper deals with the two dimensional unsteady, hydromagnetic mixed convection flow in the forward stagnation region of a sphere embedded in a porous medium with heat absorbing or generating, chemical reaction of order n. The aim of this paper is to study the influence of Soret effect, Dufour effect, porosity parameter and order of chemical reaction. The effects of material parameters on velocity, temperature and concentration are investigated mathematically.

3. MATHEMATICAL FORMULATION

Consider the unsteady laminar incompressible boundary layer flow of a viscous, chemically reacting, electrically conducting and heat generating/ absorbing binary fluid mixture in the forward stagnation region of a sphere embedded in a porous medium in the presence of a uniform magnetic field. The sphere is rotating with time dependent angular velocity $\omega(t)$. Figure 1 shows the configuration of the rotating sphere and the coordinate system. The fluid properties are assumed to be constant and homogeneous chemical reaction of order n takes place in the flow.

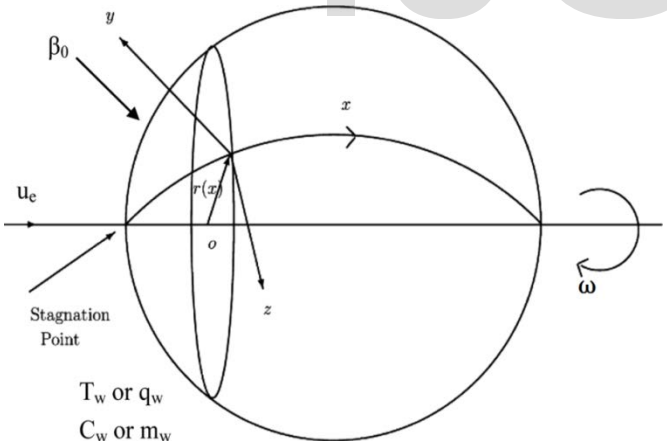

Figure 1: Physical model and the coordinate system

The velocity at the edge of the boundary later $u_e$is assumed to vary as follows:

$$u_e(x,t) = \frac{Ax}{t}, A > 0, x > 0, t > 0. \quad (1)$$

where A is the acceleration parameter. Under these assumptions as well as the Boussinesq approximation, the continuity, momentum, energy and concentration equations are given by

$$\frac{\partial(ru)}{\partial x} + \frac{\partial(rv)}{\partial y} = 0 \quad (2)$$

$$\frac{\partial u}{\partial t} + u\frac{\partial u}{\partial x} + v\frac{\partial u}{\partial y} - \left[\frac{w^2}{r}\right]\frac{dr}{dx} = \frac{\partial u_e}{\partial t} + u_e\frac{\partial u_e}{\partial x} + \nu\frac{\partial^2 u}{\partial y^2} - \frac{\sigma B_0^2}{\rho}(u-u_e) + [g\beta(T-T_\infty) + g\beta_c(C-C_\infty)] - \frac{\nu}{\kappa}(u-u_e) \quad (3)$$

$$\frac{\partial w}{\partial t} + u\frac{\partial w}{\partial x} + v\frac{\partial w}{\partial y} + \left[\frac{uw}{r}\right]\frac{dr}{dx} = \nu\frac{\partial^2 w}{\partial y^2} - \frac{\nu}{\kappa}w \quad (4)$$

$$\frac{\partial T}{\partial t} + u\frac{\partial T}{\partial x} + v\frac{\partial T}{\partial y} = \alpha\frac{\partial^2 T}{\partial y^2} + \frac{D_m K_T}{C_s C_p}\frac{\partial^2 C}{\partial y^2} + \frac{Q_0}{\rho C_p}(T-T_\infty) \quad (5)$$

$$\frac{\partial C}{\partial t} + u\frac{\partial C}{\partial x} + v\frac{\partial C}{\partial y} = D_m\frac{\partial^2 C}{\partial y^2} + \frac{D_m K_T}{T_m}\frac{\partial^2 T}{\partial y^2} - K_1(C-C_\infty)^n \quad (6)$$

where u, v, and w are the dimensional velocity components in x (longitudinal), y (transverse) and z (normal) directions respectively, t is time, r is the radial distance, T is temperature, C is concentration, ν is the kinematic viscosity of the binary fluid mixture, σ is the electrical conductivity, B_0 is the magnetic induction, ρ is the fluid density, β is the thermal expansion coefficient, β_c is compositional expansion coefficient, α is the thermal diffusivity, g is the acceleration due to gravity, K_1 is the dimensional chemical reaction parameter, C_p is the specific heat of the fluid, D_m is the mass diffusion coefficient, Q_0 is the heat generation/ absorption coefficient, K_T is the thermal diffusion ratio, C_s is the concentration susceptibility , T_m is the mean fluid temperature, κ is the permeability of porous medium, n is the order of the chemical reaction. The subscript ∞ indicates ambient condition.

The initial and boundary conditions are

$$\left.\begin{aligned} &t = 0: u(x,y,t) = u_i(x,y), v(x,y,t) = v_i(x,y), w(x,y,t) = \\ &\quad w_i(x,y), T(x,y,t) = T_i(x,y), C(x,y,t) = C_i(x,y) \\ &t > 0: u(x,y,t) = 0, v(x,y,t) = V_W, w(x,y,t) = \\ &\quad \omega(t)r, T(x,y,t) = T_W, C(x,y,t) = C_W \quad \text{at } y = 0 \\ &t > 0: u(x,y,t) = u_e(x,y), w(x,y,t) = 0, T(x,y,t) = \\ &\quad T_\infty, C(x,y,t) = C_\infty \quad \text{as } y \to \infty \end{aligned}\right\} \quad (7)$$

where V_W, T_W and C_W are the normal velocity, temperature and concentration at the wall.

Introducing the following transformations

$$\left.\begin{aligned} &u = \left[\frac{Ax}{t}\right]f'(\eta), v = -\sqrt{\frac{2\nu}{t}}Af(\eta), w = \left[\frac{Bx}{t}\right]s(\eta), r \approx x, \\ &\theta(\eta) = \frac{T-T_\infty}{T_W-T_\infty}, \phi(\eta) = \frac{C-C_\infty}{C_W-C_\infty}, u_e = \frac{Ax}{t}, \omega(t) = \frac{B}{t}, \lambda = \left(\frac{B}{A}\right)^2 = \\ &\left(\frac{w_w}{u_e}\right)^2, Pr = \frac{\nu}{\alpha}, Sc = \frac{\nu}{D_m}, \lambda_1 = \frac{Gr_x}{Re_x^2}, \lambda_2 = \frac{Gr_{C_x}}{Re_x^2}, Gr_x = \\ &\frac{g\beta(T_W-T_\infty)x^3}{\nu^2}, Gr_{C_x} = \frac{g\beta_c(C_W-C_\infty)x^3}{\nu^2}, Re_x = \frac{u_e x}{\nu}, M = \frac{\sigma B_0^2 Ax^2}{\mu Re_x}, \\ &\delta = \frac{Q_0 Ax^2}{\mu C_p Re_x}, \gamma = \frac{K_1 Ax^2}{\nu Re_x}, Da = 2\kappa, \eta = \sqrt{\frac{2}{\nu t}}y. \end{aligned}\right\} \quad (8)$$

where B is the velocity gradient at the edge of the boundary layer in the y-direction and μ is the fluid dynamic viscosity.

Using (8), equations (3) - (6) reduce to

$$f''' + Aff' + \frac{A}{2}(1 - f'^2 + \lambda s^2 + \lambda_1\theta + \lambda_2\phi) - \frac{1}{2}\left(1 - f' - \frac{\eta f''}{2}\right) - (f' - 1)\left(\frac{M}{2} + Da^{-1}\right) = 0 \quad (9)$$

$$s'' + s\left(\frac{1}{2} - Da^{-1}\right) + \frac{\eta s'}{4} + A(fs' - f's) = 0 \quad (10)$$

$$\theta'' + D_f\phi'' + \frac{Pr}{2}\left(\frac{\eta\theta'}{2} + 2Af\theta' + \delta\theta\right) = 0 \quad (11)$$

$$\phi'' + \frac{SrSc}{Pr}\theta'' + \frac{Sc}{2}\left(\frac{\eta\phi'}{2} + 2Af\phi' + \gamma\phi^n\right) = 0 \quad (12)$$

where a prime denotes differentiation with respect to η and Pr is the Prandtl number, Sc is the Schmidt number, Gr_x is the Grashof number, $Gr_{C_x}$is the modified Grashof number, $\lambda_1$and λ_2 are the buoyancy parameters, M is the magnetic field parameter, Da^{-1} is the porosity parameter, $D_f$is the Dufour number, Sr is the Soret number, δ is the heat source parameter, γ is the chemical reaction parameter and n is the order of the chemical reaction.

The initial and boundary conditions (7) are now transformed to

$$\left.\begin{aligned} f = -f_w, f' = 0, s = 1, \theta = 1, \phi = 1 \quad &\text{at} \quad \eta = 0 \\ f' = 1, s = 0, \theta = 0, \phi = 0 \quad &\text{as} \quad \eta \to \infty \end{aligned}\right\} \quad (13)$$

where $f_w = \left(\frac{V_w}{A\sqrt{2\nu/t}}\right)$ is the suction/ injection parameter such that $f_w > 0$ or $f_w < 0$ according to whether there is wall suction or injection, respectively.

The coefficients of local skin friction, local Nusselt number and local Sherwood number can be written as

$$C_{fx} = \frac{\left[2\mu\left(\frac{\partial u}{\partial y}\right)\right]_{y=0}}{\rho u_e^2} = \sqrt{\frac{8}{ARe_x}}f''(0), \qquad C_{fz} = \frac{\left[-2\mu\left(\frac{\partial w}{\partial y}\right)\right]_{y=0}}{\rho u_e^2} = -\sqrt{\frac{8\lambda}{ARe_x}}s'(0), \; Nu = \frac{-x\left(\frac{\partial T}{\partial y}\right)_{y=0}}{T_W - T_\infty} = -\sqrt{\frac{2Re_x}{A}}\theta'(0), \; Sh = \frac{-x\left(\frac{\partial C}{\partial y}\right)_{y=0}}{C_W - C_\infty} = -\sqrt{\frac{2Re_x}{A}}\phi'(0).$$

4. NUMERICAL METHOD

The system of ordinary differential equations (9) – (12) under the boundary conditions (13) have been solved numerically by using MATLAB's built in solver bvp4c.

A comparison of the present results for $f''(0), s'(0)$and $\theta'(0)$ with those reported by Anilkumar and Roy [24] is investigated and shown in table I and II. Excellent agreement between the results is obtained. This lends confidence to the numerical results to be reported subsequently.

Table I: Comparison of local surface shear stresses and heat transfer coefficient ($f''(0)$, $-s'(0)$ and $-\theta'(0)$) for different values of A and λ and $Pr = 0.7, \lambda_1 = 1, D_a^{-1} = 0, f_w = 0,\ M = 0,\ \gamma = 0, Sc = 0, D_f = 0, \delta = 0,\ \lambda_2 = 0.$

λ	A	Present work			Anilkumar and Roy (2004)		
		$f''(0)$	$-s'(0)$	$-\theta'(0)$	$f''(0)$	$-s'(0)$	$-\theta'(0)$
1	0.3	0.5008	0.0538	0.4094	0.50094	0.05390	0.40955
	0.5	0.7995	0.3035	0.4673	0.79946	0.30351	0.46743
	1.0	1.2828	0.6458	0.5895	1.28271	0.64575	0.58957
	2.0	1.9172	1.0541	0.7795	1.91728	1.05422	0.77954
3	0.3	0.7845	0.1219	0.4223	0.78468	0.12185	0.42224
	0.5	1.0988	0.3556	0.4815	1.09894	0.35565	0.48159
	1.0	1.6504	0.6960	0.6075	1.65024	0.69610	0.60766
	2.0	2.4037	1.1131	0.8037	2.40387	1.11308	0.80359

Table II: Comparison of local surface shear stresses and heat transfer coefficients ($f''(0)$, $-s'(0)$ and $-\theta'(0)$) for different values of λ and $\lambda_1$and $Pr = 0.7, A = 1, D_a^{-1} = 0, f_w = 0,\ M = 0,\ \gamma = 0, Sc = 0, D_f = 0, \delta = 0,\ \lambda_2 = 0.$

λ_1	λ	Present work			Anilkumar and Roy (2004)		
		$f''(0)$	$-s'(0)$	$-\theta'(0)$	$f''(0)$	$-s'(0)$	$-\theta'(0)$
1	1	1.2828	0.6458	0.5895	1.28271	0.64575	0.58957
	3	1.6504	0.6960	0.6075	1.65024	0.69610	0.60766
	5	1.9902	0.7376	0.6228	1.99019	0.73751	0.62273
	10	2.7617	0.8198	0.6538	2.76174	0.81974	0.65392
3	1	1.8697	0.7496	0.6298	1.86961	0.74949	0.62963
	3	2.1955	0.7851	0.6430	2.19547	0.78497	0.64316
	5	2.5047	0.8164	0.6549	2.50472	0.81630	0.65496
	10	3.2245	0.8823	0.6803	3.22435	0.88234	0.68048

5. RESULTS AND DISCUSSION

Numerical calculations have been carried out for various values of the parameters D_f, Sr, Da^{-1}, n, δ and γ. Six cases are considered:

Case I : $D_f = (0, 0.5, 1, 2), Sr = 1, \gamma = 0.5, Pr = 7, Sc = 2.6, \delta = 1, A = 1, Da^{-1} = 2, \lambda = 1, \lambda_1 = 1, \lambda_2 = 1, M = 5, n = 1.$

Case II : $D_f = 1, Sr = (0, 1, 2, 2.5), \gamma = 0.5, Pr = 7, Sc = 2.6, \delta = 1, A = 1, Da^{-1} = 2, \lambda = 1, \lambda_1 = 1, \lambda_2 = 1, M = 5, n = 1.$

Case III : $D_f = 1, Sr = 1, \gamma = 0.5, Pr = 7, Sc = 2.6, \delta = 1.8, A = 1, Da^{-1} = (1, 10, 20, 30), \lambda = 1, \lambda_1 = 1, \lambda_2 = 1, M = 5, n = 1.$

Case IV : $D_f = 1, Sr = 1, \gamma = 0.5, Pr = 7, Sc = 2.6, \delta = 1.2, A = 1, Da^{-1} = 2, \lambda = 1, \lambda_1 = 1, \lambda_2 = 1, M = 5, n = (0, 1, 2, 3).$

Case V : $D_f = 1, Sr = 1, \gamma = 0.5, Pr = 7, Sc = 2.6, \delta = (0, 1, 2, 3), A = 1, Da^{-1} = 2, \lambda = 1, \lambda_1 = 1, \lambda_2 = 1, M = 5, n = 1.$

Case VI : $D_f = 1, Sr = 1, \gamma = (0, 1, 2, 3), Pr = 7, Sc = 2.6, \delta = 1, A = 1, Da^{-1} = 2, \lambda = 1, \lambda_1 = 1, \lambda_2 = 1, M = 5, n = 1.$

The numerical results for temperature and concentration profiles are displayed in Figures (2) - (7).

Case I:

Figures 2 (a)-(b) exhibit temperature and concentration profile for various values of D_f. It is observed that the temperature and concentration decreases exponentially from their maximum values at the surface of the sphere to their minimum values at the end of the

boundary layer. It is also noticed that with an increase in the values of Dufour number D_f, the temperature increases sharply while the concentration of the binary fluid mixture decreases near the surface and the effect gets reversed after $\eta = 0.5$.

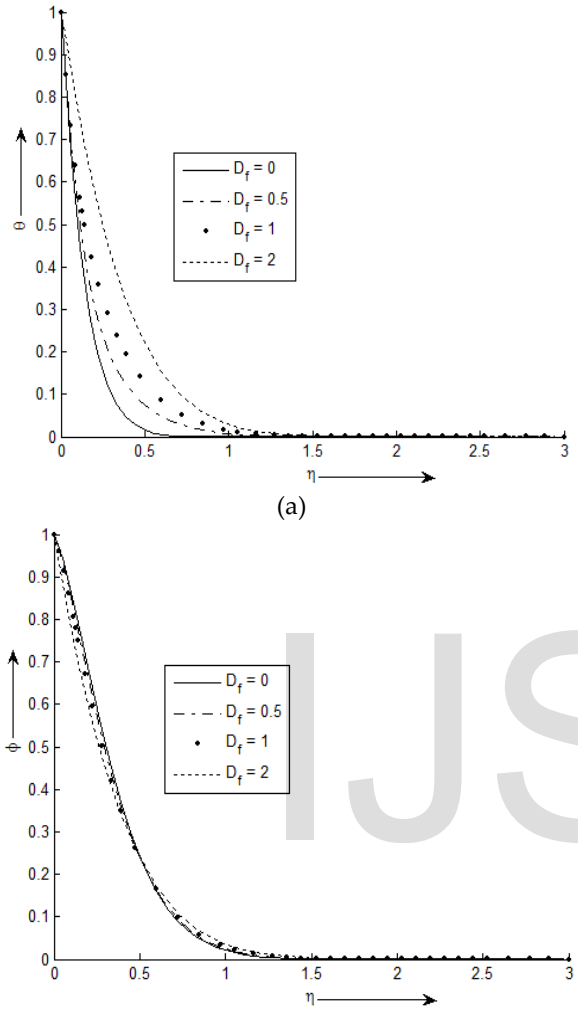

(a)

(b)

Figure 2: Effects of Dufour number D_f on (a) temperature profiles and (b) concentration profiles

Case II:

Figures 3 (a)-(b) shows temperature and concentration profile for various values of Sr. It is noticed that the temperature decreases exponentially from the maximum value at the surface to the minimum value at the end of the boundary layer. The concentration of the binary fluid mixture increases near the surface attains its maximum value at about $\eta = 0.1$ and then decreases exponentially to the minimum value at the end of the boundary layer. It is also observed that with an increase in the values of Soret number Sr, the temperature decreases sharply near the surface but the effect gets reversed after $\eta = 0.35$ while the concentration of the binary fluid mixture increases sharply.

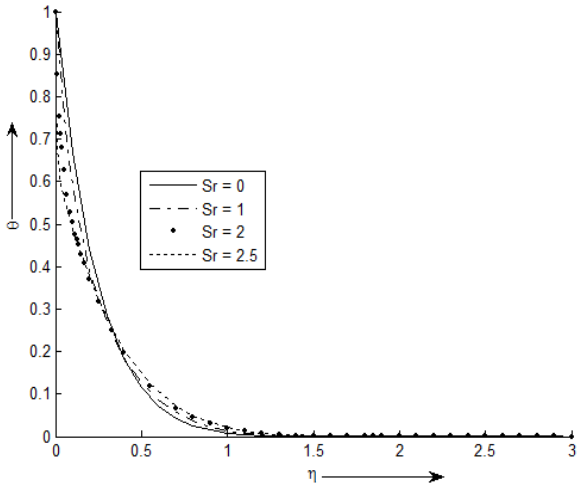

(a)

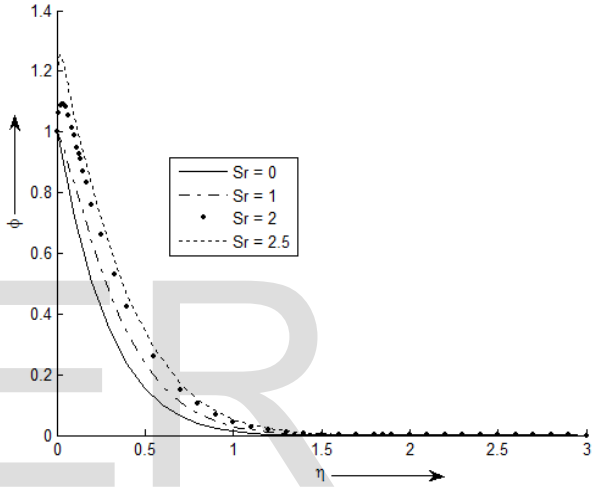

(b)

Figure 3: Effects of Soret number Sr on (a) temperature profiles and (b) concentration profiles

Case III:

Figures 4 (a)-(b) depict temperature and concentration profile for various values of Da^{-1}. It is observed that the temperature and concentration decreases exponentially from their maximum values at the surface to their minimum values at the end of the boundary layer. It is also noticed that with an increase in the values of porosity parameter Da^{-1}, the temperature and concentration decrease slightly.

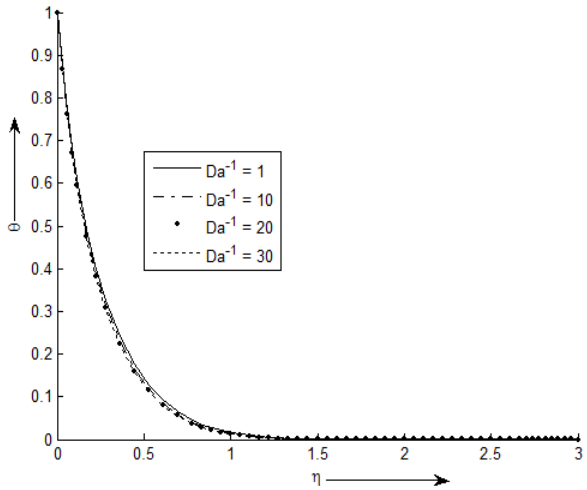

(a)

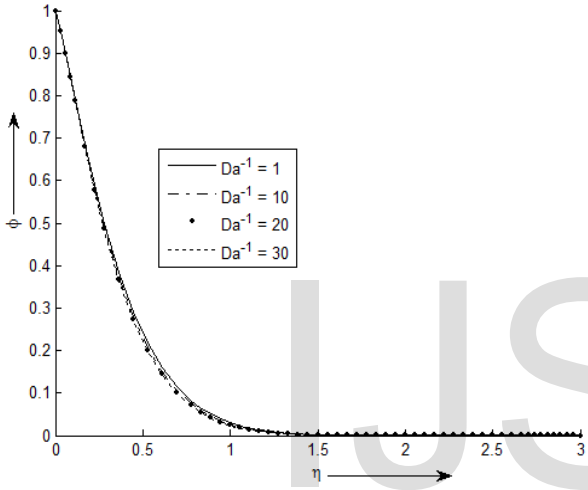

(b)

Figure 4: Effects of porosity parameter Da^{-1} on (a) temperature profiles and (b) concentration profiles

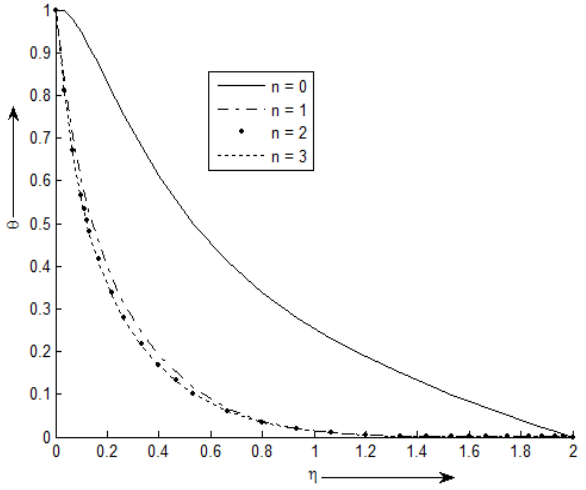

(a)

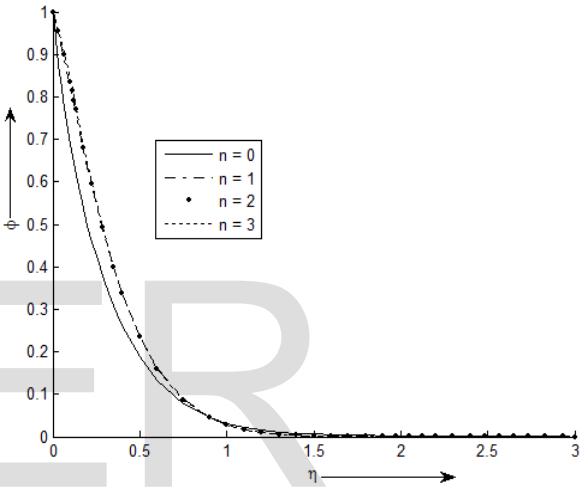

(b)

Figure 5: Effects of order of chemical reaction n on (a) temperature profiles and (b) concentration profiles

Case IV:

Figures 5 (a)-(b) exhibit temperature and concentration profile for various values of n. It is observed that the temperature and concentration decreases exponentially from their maximum values at the surface to their minimum values at the end of the boundary layer. It is also noticed that with an increase in the order of chemical reaction n, the temperature decreases sharply while the concentration of the binary fluid mixture increases.

Case V:

Figures 6 (a)-(b) depict temperature and concentration profile for various values of δ. It is observed that the temperature and concentration decreases exponentially from their maximum values at the surface to their minimum values at the end of the boundary layer. It is also noticed that with an increase in the values of heat source parameter δ, the temperature increases sharply while the concentration of the binary fluid mixture decreases slightly.

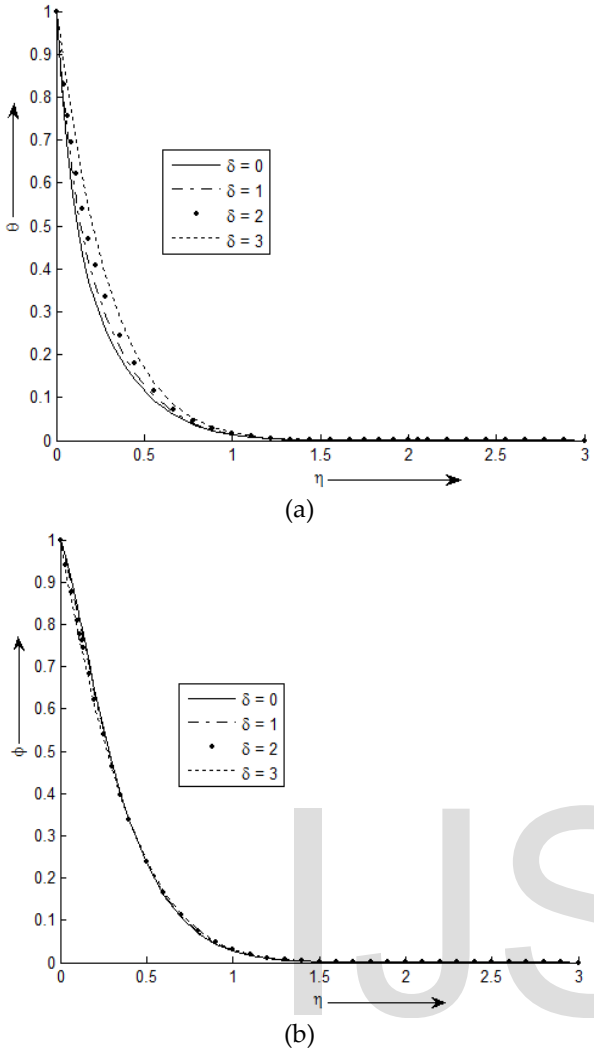

Figure 6: Effects of heat source parameter δ on (a) temperature profiles and (b) concentration profiles

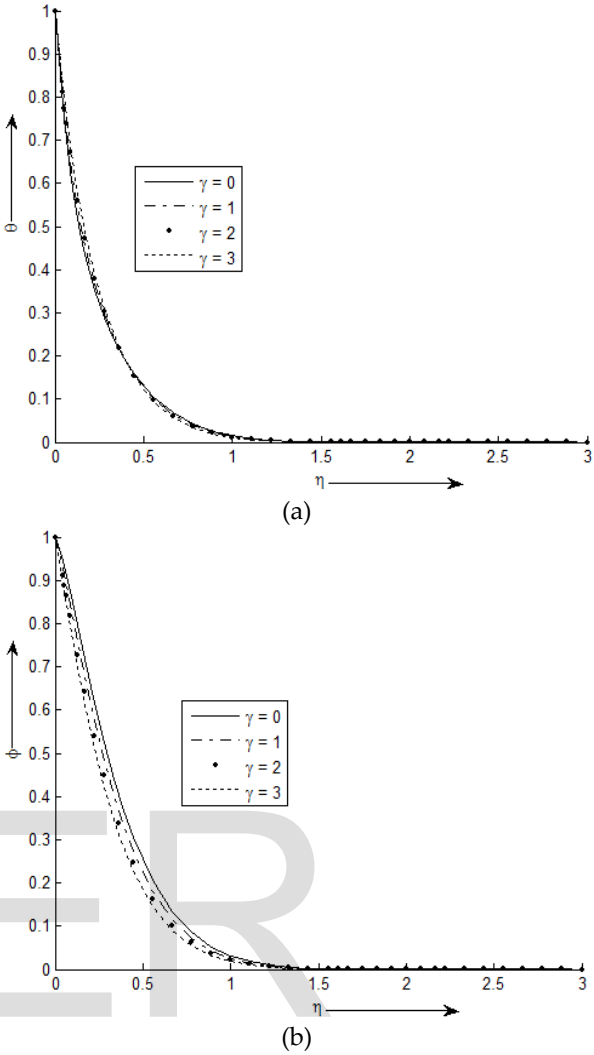

Figure 7: Effects of dimensionless chemical reaction parameter γ on (a) temperature profiles and (b) concentration profiles

Case VI:

Figures 7 (a)-(b) exhibit temperature and concentration profile for various values of γ. It is observed that the temperature and concentration decreases exponentially from their maximum values at the surface to their minimum values at the end of the boundary layer. It is also noticed that with an increase in the values of dimensionless chemical reaction parameter γ, the temperature increases near the surface but the effect gets reversed after $\eta = 1.4$ while the concentration of the binary fluid mixture decreases sharply.

Finally, with the help of the figures 8, 9 and 10, the behaviour of the local surface shear stress coefficients $\left(f''(0), -s'(0)\right)$ and the local reduced Nusselt and Sherwood numbers $\left(-\theta'(0), -\phi'(0)\right)$ are observed.

Figure 8 shows the effects of Dufour number D_f and porosity parameter Da^{-1} on the local surface shear stress coefficients $\left(f''(0), -s'(0)\right)$ and the local reduced Nusselt and Sherwood numbers $\left(-\theta'(0), -\phi'(0)\right)$. It is noticed that the local surface shear stress coefficients $\left(f''(0), -s'(0)\right)$ and the local reduced Sherwood number $\left(-\phi'(0)\right)$ increase with increasing values of either the Dufour number D_f or porosity parameter Da^{-1}. But the local reduced Nusselt number $-\theta'(0)$ increases with decreasing values of Dufour number.

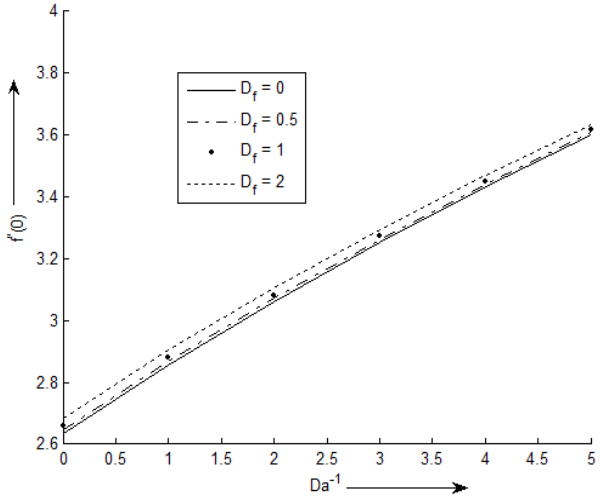

(a)

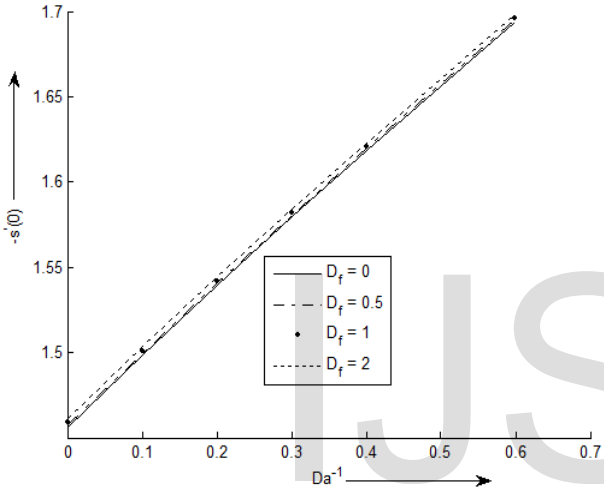

(b)

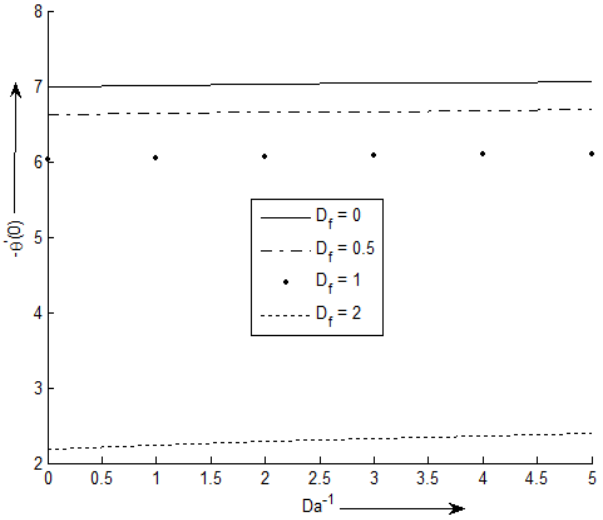

(c)

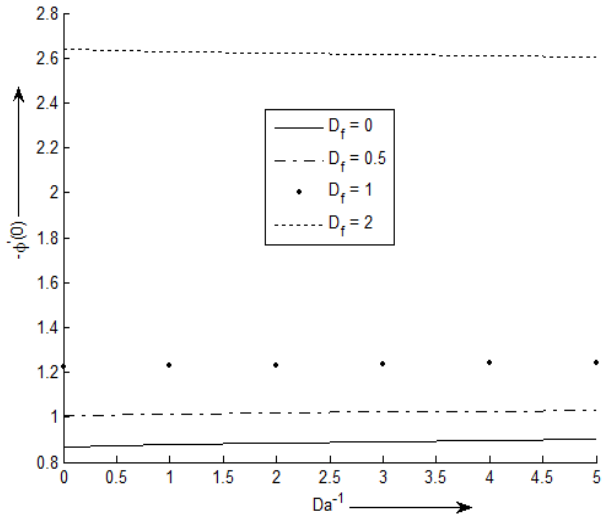

(d)

Figure 8: Effects of Dufour number D_f and porosity parameter Da^{-1} on (a) local coefficient of surface shear stress in the x-direction $f''(0)$, (b) local coefficient of surface shear stress in the y-direction $-s'(0)$, (c) local reduced Nusselt number $-\theta'(0)$ and (d) local reduced Sherwood number $-\phi'(0)$.

Figure 9 depicts the effects of Soret number Sr and order of chemical reaction n on the local surface shear stress coefficients $(f''(0), -s'(0))$ and the local reduced Nusselt and Sherwood numbers $(-\theta'(0), -\phi'(0))$. It is observed that the local surface shear stress coefficients $(f''(0), -s'(0))$ increase while the local reduced Sherwood number $(-\phi'(0))$ decreases with increasing values of Soret number Sr and decreasing order of chemical reaction . But the local reduced Nusselt number $-\theta'(0)$ increases with increasing values of either the Soret number or the order of chemical reaction.

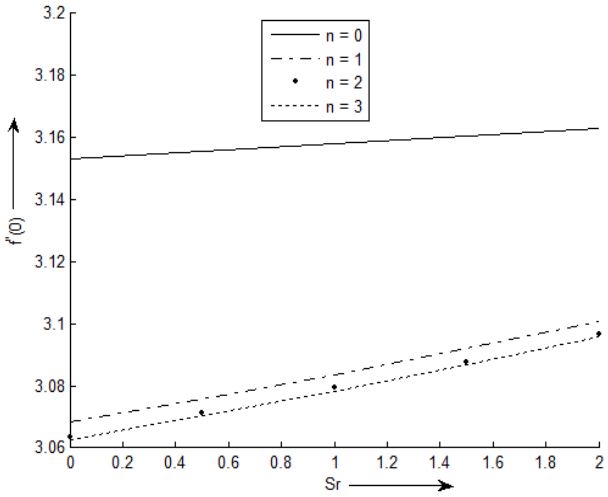

(a)

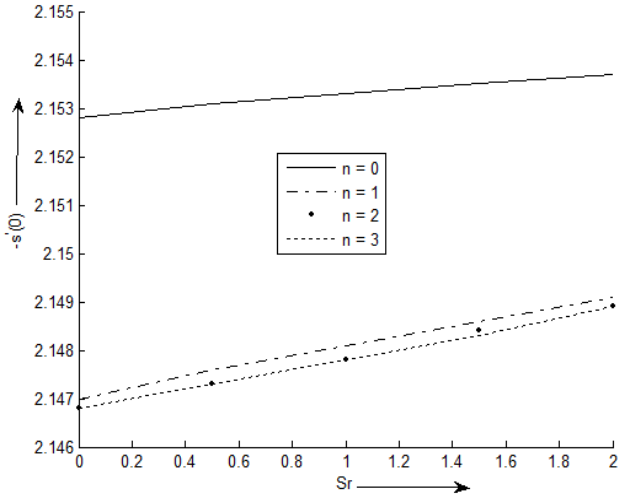

(b)

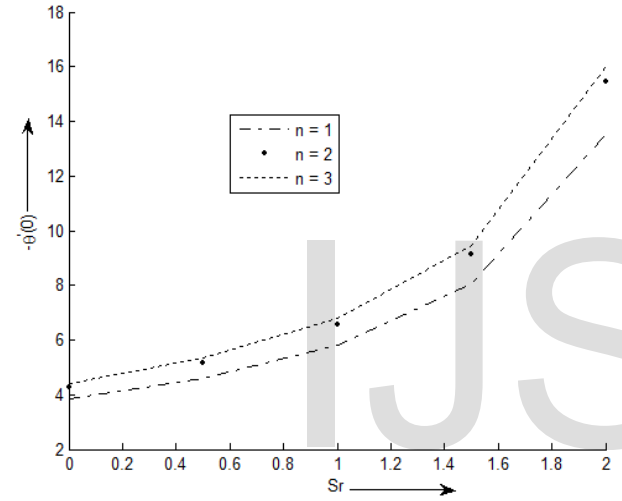

(c)

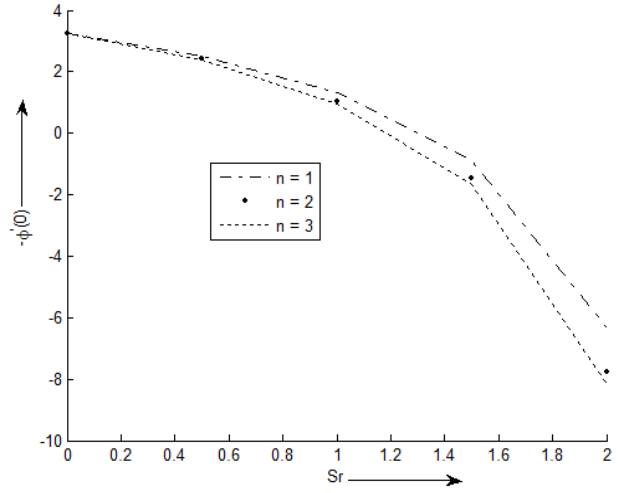

(d)

Figure 9: Effects of Soret number Sr and order of chemical reaction n on (a) local coefficient of surface shear stress in the x-direction $f''(0)$, (b) local coefficient of surface shear stress in the y-direction $-s'(0)$, (c) local reduced Nusselt number $-\theta'(0)$ and (d) local reduced Sherwood number $-\phi'(0)$.

Figure 10 exhibit the effects of heat source parameter δ and dimensionless chemical reaction parameter γ on the local surface shear stress coefficients $(f''(0), -s'(0))$ and the local reduced Nusselt and Sherwood numbers $(-\theta'(0), -\phi'(0))$. It is noticed that the local surface shear stress coefficients $(f''(0), -s'(0))$ increase while the local reduced Nusselt number $-\theta'(0)$ decreases with increasing values of heat source parameter δ and decreasing values of dimensionless chemical reaction parameter γ. But the local reduced Sherwood number $(-\phi'(0))$ increases with the increasing values of either the heat source parameter δ or the dimensionless chemical reaction parameter γ.

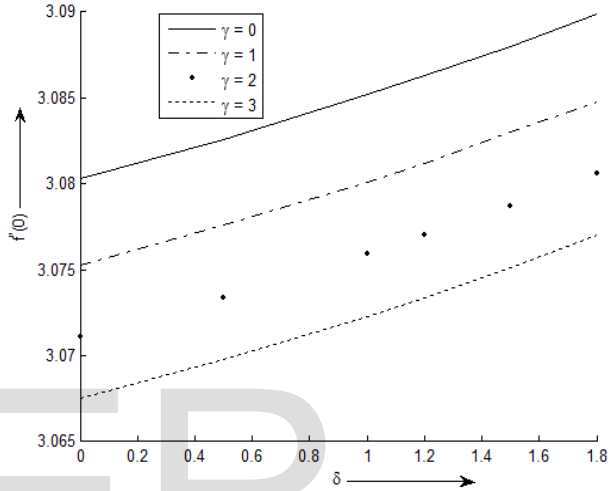

(a)

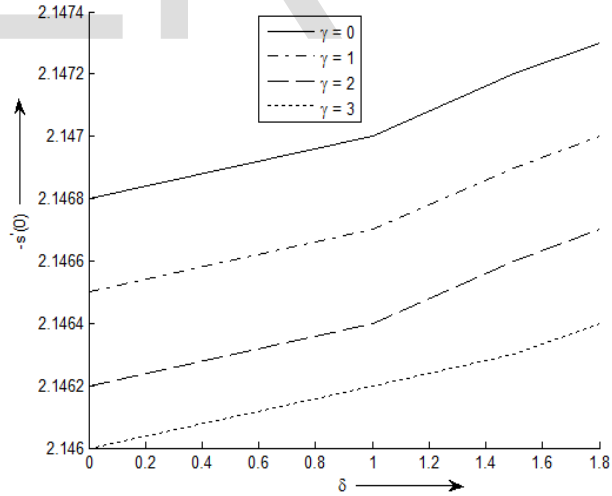

(b)

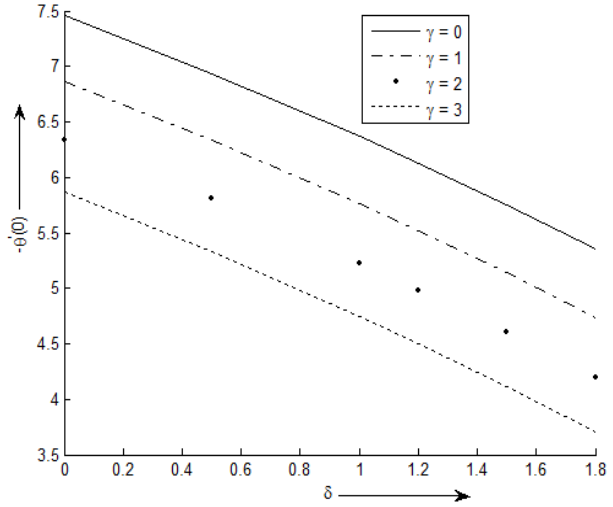

(c)

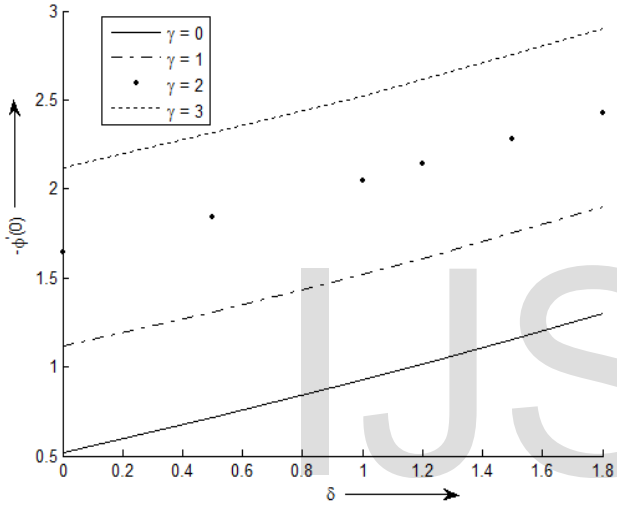

(d)

Figure 10: Effects of heat source parameter δ and dimensionless chemical reaction parameter γ on (a) local coefficient of surface shear stress in the x-direction $f''(0)$, (b) local coefficient of surface shear stress in the y-direction $-s'(0)$, (c) local reduced Nusselt number $-\theta'(0)$ and (d) local reduced Sherwood number $-\phi'(0)$.

6. CONCLUSION

The temperature of the binary fluid mixture increases with the increase of Dufour number and heat source parameter whereas decreases with the increase of porosity parameter and order of the chemical reaction. It can also be concluded that the temperature of the binary fluid mixture decreases near the surface and increases away from the surface with the increase of Soret number whereas the effect is opposite in case of dimensionless chemical reaction parameter.

Concentration of the rarer and lighter components of the binary fluid mixture increases with the increase of Soret number and order of the chemical reaction whereas decreases with increase of porosity parameter and dimensionless chemical reaction parameter. Also with the increase of Dufour number and heat source parameter, concentration decreases near the surface but the effect gets reversed away from the surface.

REFERENCES

[1] Kumar, S. K., Thacker, W. I., and Watson, L. T. (1988) Magnetohydrodynamic flow past a porous rotating disk in acircular magnetic field, *Int. J. Numer. Methods Fluids*, vol. 8, pp. 659 – 669.

[2] Kumari, M., Takhar, H. S., and Nath, G. (1993) Nonaxisymmetric unsteady motion over a rotating disk in the presence of free convection and magnetic field, *Int. J. Engng. Sci.*, vol. 31, pp. 1659 – 1668.

[3] Sparrow, E. M. and Cess, R. D. (1961) Effect of magnetic field on free convection heat transfer, *Int. J. Heat Mass Transfer*, vol. 3, pp. 267 – 274.

[4] Riley, N. (1964) Magnetohydrodynamics free convection, *J. Fluid Mech.*, vol. 18, pp. 577 – 586.

[5] Raptis, A. and Kafoussias, N. (1982) Heat transfer in flow through a porous medium bounded by an infinite vertical plate under the action of a magnetic field, *Energy Res.*, vol. 6, pp. 241 – 245.

[6] Raptis, A. and Singh, A. K. (1983) MHD free convection flow past an accelerated vertical plate, *Int. Commun. Heat Mass Transfer*, vol. 10, pp. 313 – 321.

[7] Raptis, A. A. (1986) Flow through a porous medium in the presence of a magnetic field, *Energy Res.*, vol. 10, pp. 97 – 100.

[8] Hossain, M. A. (1992) Viscous and Joule heating effect on MHD-free convection with variable plate temperature, *Int. J. Heat Mass Transfer*, vol. 35, pp. 3485 – 3487.

[9] Kafoussias, N. G. (1992) MHD free convection flow through a non-homogeneous porous medium over an isothermal cone surface, *Mech. Res. Commun.*, vol. 19, pp. 89 – 94.

[10] Takhar, H. S. and Ram, P. C. (1994) Magnetohydrodynamics free convection flow of water at 40° through a porous medium, *Int. Commun. Heat Mass Transfer*, vol. 21, pp. 371 – 376.

[11] Chamkha, A. J. (1996) Non-Darcy hydromagnetic free convection from a cone and a wedge in porous media, *Int. Commun. Heat Mass Transfer*, vol. 23, pp. 875 – 887.

[12] Sharma, B.R., Nath, Kabita and Borgohain, Debozani. (2014). "Influence of chemical reaction, heat source, Soret and Dufour effects on separation of a binary fluid mixture in MHD natural convection flow in porous media," International Journal of Computer Applications (0975 – 8887) Vol. 90 no. 2.

[13] Sharma, B. R. and Borgohain, Debozani. (2014). "Influence of the order of chemical reaction and Soret effect on mass transfer of a binary fluid mixture in

porous media," *Int. J. Inn. Res. in Science, Engg. & Tech.*, vol. 3, issue 7, pp. 14867 – 14874.

[14] Sharma, B. R. and Borgohain, Debozani. (2014). "Influence of chemical reaction, Soret and Dufour effects on heat and mass transfer of a binary fluid mixture in porous medium over a rotating disk," *IOSR Journal of Mathematics (IOSR-JM),* Vol. 10, Issue 6 Ver. III, pp. 73-78.

[15] Sharma, B.R. and Borgohain, Debozani. (2015). "Soret and Dufour Effects on Chemically Reacting MHD Mixed Convection Flow from a Rotating Vertical Cone in a Porous Medium,"

[16] Siekann, I. (1962). "The calculation of the thermal boundary layer on a rotating sphere", Z.Angew. Math. Phys., vol. 13, pp. 468–482.

[17] Chao, B. T., and Grief, R. (1974). "Laminar forced convection over rotating bodies", J. Heat Transfer, vol. 96, pp. 463–466.

[18] Lee, M. H., Jeng, D. R., and DeWitt, K. J. (1978). "Laminar boundary layer transfer over rotating bodies in forced flow", J. Heat Transfer, vol. 100, pp. 496–502.

[19] Kumari, M., and Nath, G. (1982). " Non similar incompressible boundary layer flow over a rotating sphere", Arch. Mech., vol. 34, pp. 147–164.

[20] Kumari, M., and Nath, G. (1982). "Unsteady incompressible boundary layer flow over a rotating sphere", J. Appl. Mech., vol. 49, pp. 234–236.

[21] Chen, T. S., and Mucoglu, A. (1977). "Analysis of mixed forced and free convection about a sphere", Int. J. Heat Mass Transfer, vol. 20, pp. 867–875.

[22] Takhar, H. S., Slaouti, A., Kumari, M., and Nath, G. (1998). "Unsteady free convection flow in the stagnation point region of a rotating sphere", Int. J. Non-linear Mech., vol. 33, pp. 857–865.

[23] Takhar, H. S., and Nath, G. (2000). "Self-similar solution of the unsteady flow in the stagnation point region of a rotating sphere with a magnetic field", Heat Mass Transfer, vol. 36, pp. 89–96.

[24] Anilkumar, D., and Roy, S. (2004). "Self-similar solution of the unsteady mixed convection flow in the stagnation point region of a rotating sphere", Heat Mass Transfer, vol. 40, pp. 487–493.

[25] Rashad, A.M., Chamkha, A.J. and El-Kabeir, S.M.M. (2011). "Effect of Chemical Reaction on Heat and Mass Transfer by Mixed Convection Flow About a Solid Sphere in a Saturated Porous Media," Int. J. Numerical Methods for Heat and Fluid Flow.

[26] Chamkha, A.J., Ahmed, S.E. (2012). "Unsteady MHD heat and mass transfer by mixed convection flow in the forward stagnation region of a rotating sphere at different wall conditions," *Chemical Engineering Communications*, Vol. 199, pp. 122-141.